AXIAL DEPENDENCE OF ROTATIONALLY-INDUCED BRAIN INJURIES IN FRONTAL AND OBLIQUE CRASHES

Maika, Katagiri
Jay, Zhao
TK Holdings, Inc.
United States

Paper Number 17- 0072

ABSTRACT

The occurrence and severity of traumatic brain injury (TBI) in automotive crashes has remained a major issue. Since a mechanism of TBI has been understood as head rotational kinematics, the Brain Injury Criterion (BrIC) was developed, which assesses rotational velocity about each of three axes. The aim of this study is to investigate characteristics of head rotational kinematics and their effects on TBI metrics in full frontal and frontal oblique crashes. Head rotational kinematics of the THOR dummy were analyzed utilizing 120 cases, which consisted of 0° sled tests, 15° sled tests, full frontal rigid barrier vehicle crashes (FRB), and frontal offset obliquely-oriented moving deformable barrier vehicle crashes (OBL). Six degree-of-freedom head kinematics were applied to the average male model of the Global Human Body Model Consortium. Through finite element simulations, three tissue-level metrics for TBI were calculated, namely, cumulative strain damage measure (CSDM) for diffuse brain injury, maximum principal strain (MPS) for hemorrhage and contusion, and maximum bridging vein strain (MBVS) for acute subdural hematoma. Head flexion-extension motion (ω_y) was dominant in the 0°/FRB cases, while head twist motion (ω_z) was dominant in the 15°/OBL cases. BrIC values in the 15°/OBL cases were significantly higher than the 0°/FRB cases. CSDM and MPS showed fair correlations with ω_z (R^2 = 0.45 and 0.55, respectively), while MBVS was best correlated with ω_y (R^2 = 0.50). BrIC had a good correlation with CSDM and MPS (R^2 = 0.60 and 0.64, respectively), while its correlation with MBVS was weak (R^2 = 0.16). Compared to TBI risks based on BrIC values, the risks based on CSDM values were higher in the 0°/FRB cases and lower in the 15°/OBL cases. Additional analysis demonstrated that adjustment of the relative weighting of the head rotational velocity about each axis in the BrIC formula could improve the correlation of BrIC to TBI metrics. The results indicate that CSDM and MPS are affected by head rotation regardless of the axis, while MBVS is most affected by the flexion-extension motion. MBVS correlated significantly better with y-rotation in both crash categories, though the modeling of the bridging veins may affect this trend. BrIC was proved to be a fair predictor for MPS and CSDM in the studied datasets. However, it was shown that BrIC may not be robust to a wide range of TBI as well as a wide range of load cases. This study recommends further detail analysis on how various crash modes can have different sensitivities on TBI outcomes to establish a brain injury criteria.

INTRODUCTION

Although many attempts have successfully reduced the risk of head injuries in motor vehicle crashes, the occurrence and severity of traumatic brain injury (TBI) has remained a major issue. Over the past years, the incidence of skull fracture in the field has reduced. This coincided with the reduction of the Head Injury Criterion (HIC), a metric based on linear acceleration of the head, in frontal tests of the U.S. New Car Assessment Program (NCAP). However, the incidence of TBI in frontal crashes has not reduced at a similar rate [1]. Our recent analysis of the National Automotive Sampling System – Crashworthiness Data System (NASS-CDS) from 2002 to 2014 showed that weighted estimates for TBI accounted for about 80% of severe head injuries in frontal and frontal oblique crashes. This was a population limited to seatbelt-restrained adult occupants sitting on frontal airbag-equipped front seats (see Table A1 for the restritions). Those TBI consisted of diffuse brain injury (3.9 %), Acute Subdural Hematoma (ASDH) (19.8 %), Hemorrhage (37.3 %), Contusion (11.8 %), and others (27.2 %).

Recently, Takhounts et al. [2] correlated diffuse brain injury (DAI) data with cumulative strain damage measure (CSDM) and maximum principal strain (MPS) through FE simulations with a human brain model, the simulated injury monitor (SIMon) [3] and a human head model from the Global Human Body Model Consortium (GHBMC) [4]. Based on the correlations, the Brain Injury Criterion (BrIC) was

developed as a function of angular velocities about the three axes normalized by critical values. Since injurious level of rotational velocity for CSDM and MPS showed axial dependence, a different critical value was defined for each axis. Several studies have proven BrIC to be a good predictor for rotationally-induced TBI [5]. However, it was also reported that the correlation level of BrIC to CSDM and MPS varied with the impact configurations: frontal, oblique, side, and pedestrian [5].

The National Highway Traffic Safety Administration (NHTSA) has developed a frontal offset oblique crash test configuration, which utilizes the Test device for Human Occupant Restraint (THOR) 50th percentile male metric dummy seated in the first row to represent oblique kinematics of vehicle occupants in such a crash scenario in the field [6][7]. Through the development of the test configuration, a significant head-twist motion of the THOR dummy was observed, which differs from the flexion-extension motion observed in full frontal crashes [8]. In 2015, NHTSA proposed plans for the future U.S. NCAP, which included introduction of BrIC as a supplemental head injury metric along with HIC and in addition to the adoption of the oblique offset crash test [1].

To design safety systems that effectively mitigate TBI in frontal and frontal oblique crashes, it is essential to understand the effects of head rotational kinematics on TBI. To cover a broad range of TBI in the field, three tissue-level strain based predictors were used in this study: CSDM, MPS, and maximum bridging vein strain (MBVS). While MPS was used as a predictor for DAI along with CSDM in the derivation of BrIC [2], some researches associated brain strain with hemorrhage and contusion types of TBI [9][10]. In cadaveric tests, bridging vein ruptures have been considered to cause ASDH [11]. In the frontal and frontal oblique crashes from the NASS-CDS data stated previously, DAI, hemorrhage, contusion, and ASDH accounted for about three-quarters of the severe TBI.

METHODS

A total of 120 sets of head rotational kinematics data for the THOR dummy in full frontal and frontal oblique crash tests were analyzed in this study. Six degree-of-freedom head kinematics were applied to the head model of the GHBMC 50th percentile male detailed occupant model v3.5, and through FE simulations, three TBI metrics were calculated: CSDM, MPS and MBVS. Correlations between the TBI metrics and each component of the head angular velocities were analyzed, then deviations of BrIC to the TBI metrics were also evaluated.

Analysis of head rotational kinematics from sled and vehicle crash tests with the THOR dummy

Two series of frontal and frontal oblique crash tests at 56 km/h of ΔV or corresponding severity were utilized in this study: sled tests from the NHTSA Advanced Adaptive Restraint Program [12] and the NHTSA vehicle crash test database [13]. Each test series consisted of two crash categories: 0° sled and full frontal rigid barrier (FRB) vehicle crashes for frontal crashes and 15° sled and frontal offset vehicle crashes with an obliquely oriented moving deformable barrier (OBL) [6] for frontal oblique crashes. As shown in Table 1, a total of 120 cases were extracted from the two test series based on the following criteria: THOR Mod-kit or THOR Metric dummy with angular rate sensors, no hard contact between the dummy head and the vehicle interior due to disengagement from restraints, and no data recording error. Frontal airbags and 3-point seatbelts with pretensioner were equipped in the selected cases, while side airbags were not necessarily equipped in all of them.

The crash configurations and testing dummies in these 120 cases were considered to be similar to situations where the risk of TBI would be assessed in the current and future regulations. All of the 120 cases were listed in Appendices (Table A2 and A3). Considering that the rotational velocity is a mechanism for TBI, head rotational kinematics of the THOR dummy in the selected cases were analyzed in terms of absolute maximum of rotational velocity about each axis as well as BrIC shown in Eqation (1).

$$BrIC = \sqrt{\frac{max|\omega_x|^2}{\omega_{xC}} + \frac{max|\omega_y|^2}{\omega_{yC}} + \frac{max|\omega_z|^2}{\omega_{zC}}} \qquad (1)$$

where ω_{xC} is 66.25 rad/s, ω_{yC} is 56.45 rad/s, and ω_{zC} is 42.87 rad/s [2].

Table 1.
Configurations of the sled and vehicle crash tests

Test series		Speed (km/h)	*N*
Sled	0°	56 (ΔV)	31
	15°	56 (ΔV)	28
Vehicle	FRB	56	3
	OBL	90	58

Simulations of brain injury metrics with the GHBMC FE head model

Six degree-of-freedom head kinematic data from the 120 experimental head impacts were processed and applied to the rigid skull of the GHBMC head model (Figure 1) as prescribed motion for calculation of three strain-based TBI metrics: CSDM, MPS, and MBVS. Linear accelerations and angular velocities, which were measured with respect to a local coordinate system defined by the head anatomical axes with an origin fixed at the head center-of-gravity, were filtered to channel frequency class (CFC) 1000 (1650 Hz) and 60 (100 Hz) respectively. The kinematics were applied to the head model in its local coordinate system that was consistent with the testing dummies. The head model was previously validated for skull force, relative brain-skull motion, and brain pressure using experimental data on cadavers [4].

In this study, CSDM and MPS were calculated based on strain in the five regions of the model: Cerebrum, Cerebellum, Brain stem, Basal Ganglia, and Thalamus. CSDM is the cumulative volume fraction of the brain experiencing a threshold of maximum principal strain. In this study, a threshold of 0.25 was used as in the BrIC derivation [2] as well as in Gabler et al. [5]. MPS is the 100th%ile of maximum principal strain occurring in the brain. Takhounts et al. [2] used CSDM with 0.25 of the threshold and 100th%ile of MPS to comapre SIMon and the GHBMC model. In the model, bridging veins in the superior sagittal sinus are represented by 11 one-dimensional elastic beams on the left and right side of the brain surface as shown in Figure 1. However, the beam failure mechanism and corresponding risk functions for ASDH had not been defined for the model. The maximum positive strain (tension) among the 11 beams was monitored in this study as the maximum bridging vein strain (MBVS). FE simulations were performed using LS-DYNA (v971 R6.1.2, double precision; LSTC, Livermore, CA).

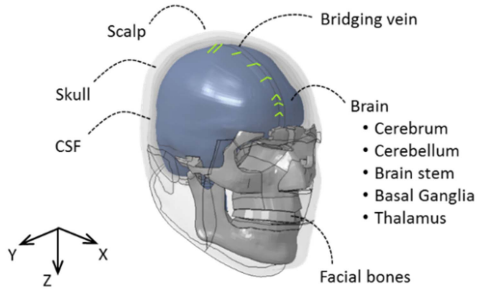

Figure 1. Global Human Body Model Consortium Male 50th percentile Head Model.

Analysis of correlations between head rotation and simulated brain injury metrics

Correlations between the TBI metrics and absolute maximum rotational velocity of the head about each axis as well as BrIC were assessed using R^2 coefficient of determination as shown in Equation (2). The value of R^2 gets closer to 1 when the data fits better to the correlation than to the simple average.

$$R^2 = 1 - \frac{\sum(Y_i - \hat{Y}_i)^2}{\sum(Y_i - \bar{Y})^2} \quad (2)$$

where Y_i is the ith dependent variable, $\hat{Y}_i$ is the ith fitted value, and $\bar{Y}$ is the mean of the dependent variable.

Scatter plots between CSDM or MPS from the simulations and BrIC were overlaid with the original correlations in Takhounts et al. [2]. Takhounts et al. [2] derived the correlations between the TBIs and BrIC (Equations (3) and (4)) through numerical simulations with SIMon. In this study, the TBI valuable of each original correlation was substituted by the relationship between each TBI value of SIMon and the GHBMC model (Equations (5) and (6)), which were also given in Takhounts et al. [2].

$$BrIC(CSDM) = 1.08 * CSDM^{SIMon} + 0.52 \quad (3)$$

$$BrIC(MPS) = 1.19 * MPS^{SIMon} \quad (4)$$

$$CSDM^{GHBMC} = 0.91 * CSDM^{SIMon} \quad (5)$$

$$MPS^{GHBMC} = 0.93 * MPS^{SIMon} \quad (6)$$

The risk of AIS 4+ was evaluated based on CSDM and MPS from the simulations and BrIC respectively with the risk functions (Equations (7-10)) in Takhounts et al. [2]. The risk functions for the TBIs (Equations (7) and (8)), which were originally derived for SIMon, were converted for the GHBMC model by substituting the valuable of each TBI with Equations (5) and (6).

$$P_{\text{AIS 4}}^{CSDM} = 1 - \mathrm{e}^{-\left(\frac{CSDM^{SIMon}}{0.60}\right)^{1.8}} \quad (7)$$

$$P_{\text{AIS 4}}^{MPS} = 1 - \mathrm{e}^{-\left(\frac{MPS^{SIMon}}{1.01}\right)^{2.84}} \quad (8)$$

$$P_{\text{AIS 4}}^{BrIC(CSDM)} = 1 - \mathrm{e}^{-\left(\frac{BrIC-0.523}{0.647}\right)^{1.8}} \quad (9)$$

$$P_{\text{AIS 4}}^{BrIC(MPS)} = 1 - \mathrm{e}^{-\left(\frac{BrIC}{1.204}\right)^{2.84}} \quad (10)$$

RESULTS

Head rotational kinematics of the THOR dummy

Distributions for each crash category of the test series are shown in Figure 2. In the 0°/FRB cases, the average rotational velocity about y-axis, $max|\omega_y|$ was observed to be largest. On the other hands, in the 15°/OBL cases, the average rotational velocity about z-axis, $max|\omega_z|$ was largest. The average of $max|\omega_y|$ in each crash category was in the same range, while $max|\omega_x|$ and $max|\omega_z|$ as well as BrIC values in the 15°/OBL cases were significantly higher than those in the 0°/FRB cases. The sled tests and the vehicle crash tests showed the same trends in terms of absolute maximum rotational velocity about each axis as well as BrIC values (Figure A1).

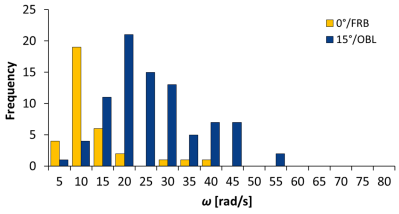

(a) $max|\omega_x|$

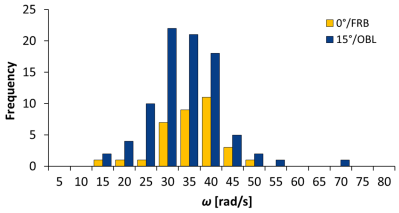

(b) $max|\omega_y|$

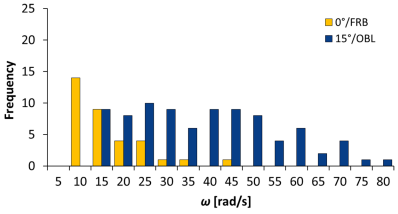

(c) $max|\omega_z|$

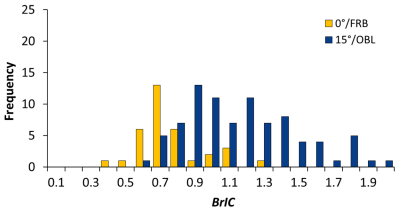

(d) BrIC

Figure 2. Distribution of absolute maximum rotational velocity about each axis and BrIC values.

Brain injury metrics in the GHBMC FE head model simulations

In the FE simulations, CSDM, MPS and bridging vein strain increased along with angular velocity regardless of the axis. Figure 3 shows a 0°/FRB and a 15°/OBL cases. While y-axis head rotation (flexion-extension) was dominant in the 0°/FRB case, rotation about all axis was observed in the 15°/OBL case. The MPS value rose at the time when rotational velocity about any axis initially increased and continued to increase along with the increase of rotational velocity of each axis, which made its time history synchronize well with that of BrIC. On the other hand, the CSDM value rose about the time when the rotational velocity was about to reach to the first peak and continued to increase in a more gradual manner than that of MPS. Bridging vein strain rose along with angular velocity about any axis. The vein beams in the anterior area (#1 to #3) and in the parietal and posterior areas (#5 to #11) tended to be strained in the opposite direction.

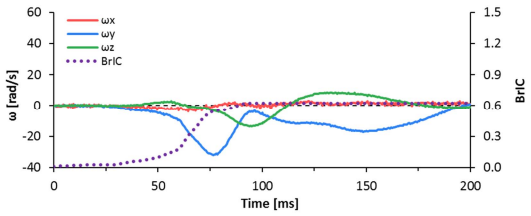

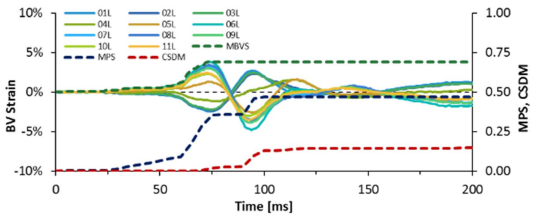

(a) 0°/FRB

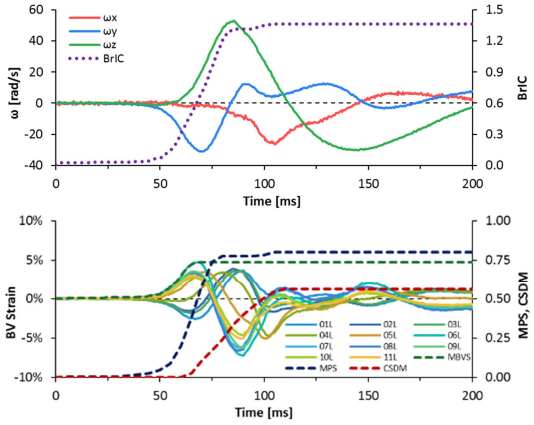

(b) 15°/OBL

Figure 3. Head rotational velocity applied to the head model and BrIC (top) and CSDM, MPS, MBVS and strain of bridging veins in the left side of the brain (bottom).

Correlations of head rotation to TBI metrics

Different trends in the correlations between the TBI metrics and head rotation about each axis as well as BrIC were observed for each TBI metric. As R^2 values in Table 2 show, MPS and CSDM showed better correlations with $max|\omega_z|$, while MBVS was significantly better correlated with $max|\omega_y|$. BrIC had a good correlation with MPS and CSDM, while its correlation with MBVS was poor.

As shown in Figure 4, for CSDM and MBVS, significant numbers of the 0°/FRB cases were plotted below the correlation lines, while significant numbers of the 15°/OBL cases were plotted above. This difference can be seen from the correlation trend for each crash category. Additionally, the correlation line for MPS was close and parallel to the original correlation at the range of the MPS values, while the correlation line for CSDM was steeper than the original one. Compared to TBI risks based on BrIC values, the risks based on CSDM values were higher in most of the 0°/FRB cases and lower in majority of the 15°/OBL cases as show in Figure 5.

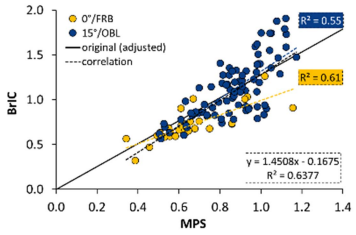

(a) MPS

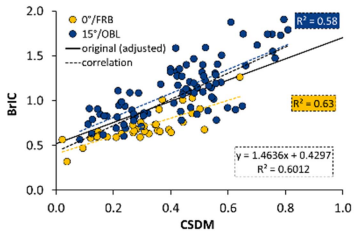

(b) CSDM

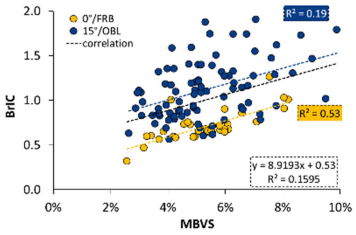

(c) MBVS

Figure 4. Scatter plots for correlations between the TBIs and BrIC values with the original correlations of MPS and CSDM [2] for the GHBMC head model.

Table 2.
R^2 of the correlations between each TBI and absolute maximum rotational velocity of the head as well as BrIC

	$max\|\omega_x\|$	$max\|\omega_y\|$	$max\|\omega_z\|$	BrIC
MPS	0.32	0.02	0.55	0.64
CSDM	0.15	0.16	0.45	0.60
MBVS	0.01	0.50	0.04	0.16

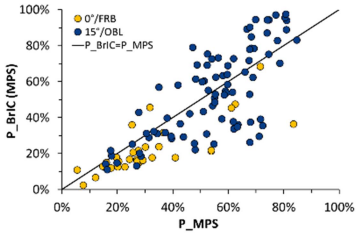

(a) MPS

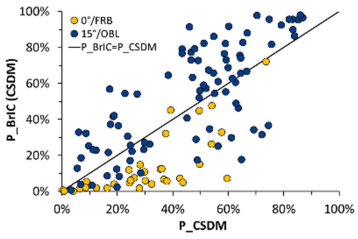

(b) CSDM

Figure 5. Scatter plots between AIS 4+ risk based on MPS or CSDM and BrIC values (Note: the risk functions for the TBIs [2] were adjusted for the GHBMC head model).

DISCUSSION

Head y-rotation was dominant in the 0°/FRB cases, where the THOR dummy move fore-aft and head flexion-extension motion is produced by relative displacement between the head and chest restrained by mainly the front airbag and seatbelts, respectively. In the 15°/OBL cases, head z-rotation was largest, which is because the THOR dummy moves laterally and longitudinally and head twist motion is generated by contacting the front airbag. Additionally, rotational motion about all axes in the 15°/OBL cases was similar to or larger than the 0°/FRB cases, which resulted in higher BrIC in the 15°/OBL cases, where the dummy engages with the restrains in a limited manner. It should be noted that the sled tests and the vehicle crash tests were common in averages and distributions of absolute maximum rotational velocities of the head, which made it reasonable to merge the two series of tests and analyze correlations to the TBI metrics together.

MPS and CSDM were influenced by head rotation regardless of the axis. The time history of MPS was well synchronized with BrIC. Combined with the nature of MPS, it was indicated that rotational velocity is a mechanism of causing strain in the brain. On the other hand, CSDM rose later than MPS with a gradual increasing slope. This trend coincided with the fact that CSDM assesses brain strain cumulatively rather than at each moment like MPS does. It can be assumed that the structural geometry of the head might affect this trend. The falx and tentorium, membranes separating the cerebral hemisphere sagittally and from the cerebellum respectively, could constrain displacement of the brain and induce its deformation.

The bridging vein beams were strained along with head rotational velocity regardless of the axis. Since head y-rotation was dominant in the 0°/FRB cases, it was clearly observed that the time history trend of bridging vein strain was consistent with that of rotational velocity about the y-axis. In the 15°/OBL cases, where x- and z-rotation in addition to y-rotation occurred, the time history trend of bridging vein strain was not necessarily consistent with the y-rotational velocity. However, MBVS was correlated significantly better with y-rotation only, though the modeling of the bridging veins may affect this trend. The bridging vein beams in the head model connect the brain surface and the skull on the sagittal plane generally, which might make it tend to be more sensitive to the sagittal rotation. Length and angle of the beams varied in the location of the head, which might cause the direction of strain: tension or extension.

BrIC was shown to be a good predictor for MPS and CSDM. However, the correlation to MBVS was poor and plots of the simulated MBVS to the measured value of BrIC were widely scattered over the correlation, which might suggest that the BrIC formula may not predict ASDH well. Although the BrIC formula was derived based on its correlations with CSDM and MPS as predictors for diffuse brain injury, it would be expected to cover a broad range of or common TBIs in automotive crashes. Further studies are required on whether if bridging vein strain is an effective predictor for ASDH as well as CSDM and MPS could cover a broad range of TBI. Additionally, trends of the correlations between BrIC and the TBI metrics was dependent on the crash category, which indicate that BrIC might not be robust to crash configurations. Further more, the correlation level in this study was lower than those reported in other studies [2][5], where larger datasets from multiple crash configurations with multiple testing dummies were used. Generally speaking, the larger datasets were used, the higher correlation level could be expected. Although the total size of studeid dataset was smaller, it sololy consisted of the THOR dummy, which has a higher biofidelity.

Furthermore, the original correlations of BrIC generally understated CSDM and MBVS from the 0°/FRB cases and overstated those from the 15°/OBL cases, where y-rotation and z-rotation of the head was significant respectively. Combined with the observation above stating BrIC's dependency on crash configuraions, a further analysis was motivated to clarify which axis of the critical rotational velocities of the BrIC formula influenced this trend. The BrIC value of each case was re-calculated with

different sets of the critical values changing from 30 rad/s to 75 rad/s every 1 rad/s. Figure 6 shows scatter plots of BrIC values with the adjusted sets of the critical values, which minimized R^2 best among all of the different sets. For both CSDM and MBVS, ω_{yC} was smallest rather than ω_{zC} in the BrIC formula, which indicated that flexion-extension motion was understated and twist motion was overstated to predict TBI by the formula. However, it should be noted that the analysis described in this study was not taken to suggest a new set of the critical values. Instead, this observation suggests further reconsideration of the relative weighting of the head rotational velocity about each axis in the BrIC formula similar to Yanaoka et al. [14].

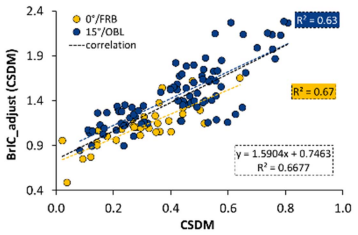

(a) CSDM

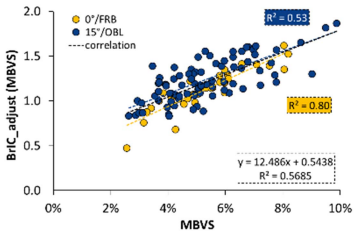

(b) MBVS

Figure 6. Scatter plots for correlations between the TBIs and BrIC values with adjusted critical values (ω_{xC} = 75, ω_{yC} = 32, and ω_{zC} = 38 rad/s for CSDM, ω_{xC} = 75, ω_{yC} = 30, and ω_{zC} = 75 rad/s for MBVS).

CONCLUSIONS

In 0°/FRB and 15°/OBL sled frontal crashes, CSDM and MPS are affected by multiple axes of head rotation, while MBVS is most affected by the flexion-extension motion. BrIC was proved to be a fair predictor for MPS and CSDM in the studied datasets. However, it was shown that BrIC may not be robust to a wide range of TBI as well as a wide range of load cases. This study reccomends further detail analysis on how various crash modes can have different sensitivities on TBI outcomes to establish a brain injury criteira.

REFERENCES

[1] National Highway Traffic Safety Administration (NHTSA). 2015. New Car Assessment Program; Request for comments notice. Washington DC: National Highway Traffic Safety Administration, US Department of Transportation; NHTSA-2015-0119.

[2] Takhounts E, Craig MJ, Moorhouse K. Mcfadden J, Hasija V. 2013. Development of brain injury criteria (BrIC). Proc. 57th Stapp Car Crash Conference, SAE Paper No. 2013-22-0010, 243-266.

[3] Takhounts E, Hasija V, Ridella SA. TANNOUS RE, Campbell JQ, Malone D, Danelson K, Stitzel J, Rowson S, Duma S. 2008. Investigation of traumatic brain injuries using the next generation of simulated injury monitor (SIMon) finite element head model. Proc. 52nd Stapp Car Crash Conference, SAE Paper No. 2008-22-0001, 1-32.

[4] Mao H, Zhang L, Jiang B. Genthikatti VV, Jin Z, Zhu F, Makwana R, Gill A, Jandir G, Singh A, Yang KH. 2013. Development of a finite element human head model validated with forty nine loading cases from experimental and real world impacts. J Biomech Eng., 135(11):111002.

[5] Gabler LF, Crandall JR, Panzer MB. 2016. Assessment of kinematics brain injury metrics for predicting strain responses in diverse automotive impact conditions. Ann Biomed Eng., 44(12):3705-3718.

[6] Saunders J, Craig M, Suway J. 2011. NHTSA's test procedure for small overlap/oblique crashes. Paper presented at: 22nd International Technical Conference on the Enhanced Safety of Vehicles (ESV); June 13- 16; Washington, D.C., USA.

[7] Rudd R. 2016. Investigating a relationship between standardised crash classification and occupant kinematics in real-world frontal crashes. Paper presented at: International Research Council of Biomechanics (IRCOBI) Conference; September 14-16; Malaga, Spain.

[8] Saunders J, Parent D, Ames E. 2015. NHTSA oblique crash test results: vehicle performance and occupant injury risk assessment in vehicles with small overlap countermeasures. Paper presented at: 24th International Technical Conference for the Enhanced Safety of Vehicles (ESV); June 8-11; Gothenburg, Sweden.

[9] Nusholtz GS, Wylie B, Glascoe LG. 1995. Cavitation/boundary effects in a simple head

impact model. Aviation, space, and environmental medicine. 66(7), 661-667.

[10] Shatsky SA, Alter WA, Evans DE. Armbrustmacher VW, Clark G, Earle KM. 1974. Traumatic distortions of the primate head and chest: correlation of biomechanical, radiological and pathological data. Proc. 18th Stapp Car Crash Conference, SAE Paper No. 741186, 3707-3723.

[11] Depreitere B, Van Lierde C, Sloten JV, Van Audekercke R, Van der Perre G, Plets C, Goffin J. 2006. Mechanics of acute subdural hematomas resulting from bridging vein rupture. J Neurosurg, 104(6):950-6.

[12] Cyliax B, Scavnicky M, Muller I, Zhao J, Hiroshi A. 2016. Advance adaptive restraint program – individualization of occupant safety systems with a focus on oblique impact. Paper presented at: SAE Government/Industry Meeting, January 20-22, Washington, D.C., USA.

[13] National Highway Traffic Safety Administration (NHTSA). 2016. NHTSA Vehicle Crash Test Database. Available at: http://www-nrd.nhtsa.dot.gov/database/veh/veh.htm. Accessed October 12, 2016.

[14] Yanaoka T, Dokko Y, Takahashi Y. 2015. Investigation on an injury criterion related to traumatic brain injury primarily induced by head rotation. Paper presented at: 2015 SAE World Congress; Detroit, SAE Paper No. 2015-01-1439.

APPENDICES

Table A1.
Restrictions for interrogating NASS CDS database

Parameter	Restriction
Event Year	2002-2014
Model Year	2000-2014
PDOF	11, 12, 01
CDC	**FL****, **FY****
Rollover	Excluded
Occupant age	15-100 years old
Sex	Male, female
Seat position	Front seats
Seatbelt	Belted
Front airbag	Equipped
Region of injury	Head

Table A2.
List of 59 of sled tests analyzed in this study: D (driver), P (passenger), FS (far-side), and NS (near-side).

Test ID	THOR	Sled Angel	Seat
BDSJ0130	Mod-kit	0°	D
BDSJ0141	Mod-kit	0°	D
BDSJ0155	Mod-kit	0°	D
BDSJ0173	Mod-kit	0°	D
BDSJ0179	Mod-kit	0°	D
BDSK0066	Mod-kit	0°	D
BDSK0108	Mod-kit	0°	D
BDSK0116	Mod-kit	0°	D
BDSK0122	Mod-kit	0°	D
BDSK0123	Mod-kit	0°	D
BDSK0125	Mod-kit	0°	D
BDSK0172	Mod-kit	0°	D
BDSK0173	Mod-kit	0°	D
BDSK0192	Mod-kit	0°	D
BDSK0202	Mod-kit	0°	D
BDSK0287	Mod-kit	0°	D
BDSK0297	Mod-kit	0°	D
BDSK0372	Mod-kit	0°	D
BDSL0011	Mod-kit	0°	D
BDSL0056	Mod-kit	0°	D
BDSL0068	Mod-kit	0°	D
BDSJ0137	Mod-kit	0°	P
BDSJ0140	Mod-kit	0°	P
BDSJ0162	Mod-kit	0°	P
BDSJ0184	Mod-kit	0°	P
BDSK0088	Mod-kit	0°	P
BDSK0174	Mod-kit	0°	P
BDSK0371	Mod-kit	0°	P
BDSL0009	Mod-kit	0°	P
BDSL0022	Mod-kit	0°	P
BDSL0080	Mod-kit	0°	P
BDSJ0286	Mod-kit	15°	D (FS)
BDSK0021	Mod-kit	15°	D (FS)
BDSL0073	Mod-kit	15°	D (FS)
BDSL0074	Mod-kit	15°	D (FS)
BDSJ0136	Mod-kit	15°	P (FS)
BDSJ0142	Mod-kit	15°	P (FS)
BDSK0115	Mod-kit	15°	P (FS)
BDSK0119	Mod-kit	15°	P (FS)
BDSK0255	Mod-kit	15°	P (FS)
BDSK0376	Mod-kit	15°	P (FS)
BDSL0134	Mod-kit	15°	P (FS)
BDSJ0133	Mod-kit	15°	D (NS)
BDSJ0143	Mod-kit	15°	D (NS)
BDSJ0154	Mod-kit	15°	D (NS)
BDSJ0180	Mod-kit	15°	D (NS)
BDSJ0185	Mod-kit	15°	D (NS)
BDSK0109	Mod-kit	15°	D (NS)

BDSK0120	Mod-kit	15°	D (NS)
BDSK0124	Mod-kit	15°	D (NS)
BDSK0256	Mod-kit	15°	D (NS)
BDSK0270	Mod-kit	15°	D (NS)
BDSK0306	Mod-kit	15°	D (NS)
BDSK0341	Mod-kit	15°	D (NS)
BDSK0389	Mod-kit	15°	D (NS)
BDSL0021	Mod-kit	15°	D (NS)
BDSL0028	Mod-kit	15°	D (NS)
BDSL0079	Mod-kit	15°	D (NS)
BDSL0112	Mod-kit	15°	D (NS)

Table A3.
List of 61 of vehicle crash tests used in this study: D (driver), P (passenger), FS (far-side), and NS (near-side).

Test ID	THOR	Crash Test	Seat
9334	Metric	FRB	D
9336	Metric	FRB	D
9337	Metric	FRB	D
9354	Mod-Kit	OBL	D (FS)
9478	Mod-Kit	OBL	D (FS)
9480	Mod-Kit	OBL	D (FS)
9483	Mod-Kit	OBL	D (FS)
9727	Metric	OBL	D (FS)
8478	Mod-Kit	OBL	P (FS)
8488	Mod-Kit	OBL	P (FS)
8788	Mod-Kit	OBL	P (FS)
8875	Mod-Kit	OBL	P (FS)
9135	Mod-Kit	OBL	P (FS)
9140	Mod-Kit	OBL	P (FS)
9146	Mod-Kit	OBL	P (FS)
9148	Mod-Kit	OBL	P (FS)
9149	Mod-Kit	OBL	P (FS)
9152	Mod-Kit	OBL	P (FS)
9476	Mod-Kit	OBL	P (FS)
9479	Mod-Kit	OBL	P (FS)
9481	Mod-Kit	OBL	P (FS)
7467	Mod-Kit	OBL	D (NS)
7851	Mod-Kit	OBL	D (NS)
7852	Mod-Kit	OBL	D (NS)
8475	Mod-Kit	OBL	D (NS)
8476	Mod-Kit	OBL	D (NS)
8477	Mod-Kit	OBL	D (NS)
8478	Mod-Kit	OBL	D (NS)
8488	Mod-Kit	OBL	D (NS)
8787	Mod-Kit	OBL	D (NS)
8788	Mod-Kit	OBL	D (NS)
8789	Mod-Kit	OBL	D (NS)
8791	Mod-Kit	OBL	D (NS)
8875	Mod-Kit	OBL	D (NS)
8882	Mod-Kit	OBL	D (NS)
9122	Mod-Kit	OBL	D (NS)
9126	Mod-Kit	OBL	D (NS)
9127	Mod-Kit	OBL	D (NS)
9137	Mod-Kit	OBL	D (NS)
9138	Mod-Kit	OBL	D (NS)
9139	Mod-Kit	OBL	D (NS)
9140	Mod-Kit	OBL	D (NS)
9143	Mod-Kit	OBL	D (NS)
9145	Mod-Kit	OBL	D (NS)
9146	Mod-Kit	OBL	D (NS)
9148	Mod-Kit	OBL	D (NS)
9149	Mod-Kit	OBL	D (NS)
9151	Mod-Kit	OBL	D (NS)
9152	Mod-Kit	OBL	D (NS)
9211	Mod-Kit	OBL	D (NS)
9214	Mod-Kit	OBL	D (NS)
9228	Mod-Kit	OBL	D (NS)
9476	Mod-Kit	OBL	D (NS)
9479	Mod-Kit	OBL	D (NS)
8998	Mod-Kit	OBL	P (NS)
8999	Mod-Kit	OBL	P (NS)
9042	Mod-Kit	OBL	P (NS)
9354	Mod-Kit	OBL	P (NS)
9478	Mod-Kit	OBL	P (NS)
9482	Mod-Kit	OBL	P (NS)
9727	Metric	OBL	P (NS)

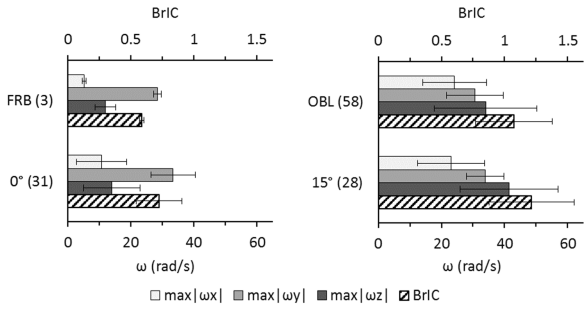

Figure A1. Averages of absolute maximum rotational velocity about each axis and BrIC values with the error bars representing the standard deviations, with numbers of tests in parentheses.